NASA
Technical Memorandum 107169

Army Research Laboratory
Technical Report ARL–TR–1061

Strength Degrading Mechanisms for CVD SCS–6 SiC Fibers in Argon Environments

Ramakrishna T. Bhatt
Vehicle Propulsion Directorate
U.S. Army Research Laboratory
Lewis Research Center
Cleveland, Ohio

and

David R. Hull
Lewis Research Center
Cleveland, Ohio

Prepared for the
17th Annual Conference on Composites, Materials, and Structures
sponsored by the American Ceramic Society
Cocoa Beach, Florida, January 10–15, 1993

National Aeronautics and
Space Administration

STRENGTH DEGRADING MECHANISMS FOR CVD SCS-6 SIC FIBERS IN ARGON ENVIRONMENTS

Ramakrishna T. Bhatt
Vehicle Propulsion Directorate
U.S. Army Research Laboratory
Lewis Research Center
Cleveland, Ohio 44135

and

David R. Hull
National Aeronautics and Space Adminstration
Lewis Research Center
Cleveland, Ohio 44135

SUMMARY

The room temperature tensile strengths of chemically vapor deposited SCS-6 silicon carbide fibers were measured after 1 to 400 hr heat-treatments in 0.1 MPa argon at temperatures to 2100 °C. The fibers heat treated for 1 hr above 1400 °C and those heat treated for 400 hr above 1300 °C showed strength degradation. Scanning and transmission electron microscopic examination of the degraded fibers showed formation of a recrystallization region within the outer zone of the SiC sheath and the growth of SiC particles in the carbon-rich surface coating. The activation energies for the growth of the recrystallization region and the SiC particles were ~370 and ~320 kJ/mole, respectively. Tensile strength of the fibers was found to vary as an inverse function of the recrystallized zone thickness.

INTRODUCTION

Silicon carbide fibers fabricated by a chemical vapor deposition method (CVD) have been used as a reinforcement for both metal and ceramic matrix composites. One type of CVD SiC fiber that has been quite extensively used for composite fabrication is the SCS-6 fiber manufactured by Textron Specialty Materials, Lowell, Massachusetts. This fiber offers several advantages over other commercially available SiC fibers manufactured by polymer pyrolysis, namely high as-fabricated strength, modulus, chemical purity, and the availability with a pyrolytic carbon-rich surface coating.

A schematic diagram of a typical fiber cross-section is shown in figure 1(a). The fiber is grown to a diameter of ~140 μm by depositing SiC onto a heated 37 μm diameter pyrolytic graphite coated carbon core. The SiC sheath has four distinct zones. The three inner zones (Regions C, D, and E) consist of carbon-rich β-SiC grains having slightly different aspect ratio and orientation, while the outer zone (Region B) contained nearly stoichiometric β-SiC grains (refs. 1 and 2). An approximately 3 μm thick complex carbon-rich coating (Region A) is also deposited on top of the SiC sheath for several purposes: to protect the fiber from surface damage, to serve as a sacrificial layer in titanium matrix composites, and to provide a weak interface for matrix crack deflection in some ceramic matrix composites. The approximate composition of this surface coating is shown in figure 1(b). The carbon-rich surface coating contains SiC particles whose size and distribution varies depending on the location within the coating (refs. 1 and 2).

It has been shown previously by Bhatt and Hull (ref. 3) that the SCS-6 fiber retains its as-fabricated room temperature tensile strength after 1 hr exposure in N_2, Ar, and vacuum environments at temperatures to 1400 °C. Beyond this temperature, the fiber showed strength degradation which is related to growth of SiC grains in the outer zone (Region B) of the SiC fibers. However, long term heat treatment effects on the microstructure and strength

stability have not been fully investigated. Since fiber properties play a dominant role in controlling composite properties, knowledge of the stability range and the mechanism of fiber degradation are required for designing fiber-reinforced ceramic matrix composites for advanced heat engine applications. This study had a two-fold objective: first, from a basic point of view, to study degradation behavior of SCS-6 fibers in an argon environment and relate tensile strength to recrystallization mechanisms; second, from a practical point of view, to determine long term strength stability and the upper use temperature for this fiber.

EXPERIMENTAL

Heat treatment

For heat-treatments, batches of twenty-five individual SCS-6 fibers of length 125 mm were placed in grafoil envelopes and loaded into a graphite furnace. The graphite elements and grafoil envelope were used to avoid possible oxidation of the fiber surface coating as the argon gas contained ~3 ppm of oxygen. The fibers were heat-treated under 0.1 MPa argon pressure from 1200 to 2100 °C at 200 °C intervals for 1, 10, 100, 200, and 400 hr.

Testing

The heat treated fibers were prepared for tensile testing at room temperature by forming aluminum foil clamps at their ends, leaving 50 mm as the gauge length. The aluminum foils were inserted in pneumatic grips, and the fiber specimens were pulled to failure using a tensile testing machine at a constant cross head speed of 1.3 mm/min. For each heat-treatment, the tensile strength of ten to twenty fibers was measured.

X-ray Diffraction

To determine phase stability, heat treated fibers were analyzed by x-ray diffraction (XRD). The XRD runs were made at a scanning speed of 1 deg/min using standard equipment with a Ni filter and Cu K radiation.

Microstructural Characterization

For microstructural characterization, ~2 cm long fibers, both as-received and heat-treated, were embedded in an epoxy mold. The mold was ground on diamond impregnated metal discs and then polished on a vibratory polisher using microcloth and 0.03 μm diamond slurry. The polished specimens were etched with Murakami's reagent or with a fluorocarbon plasma to delineate the grain boundaries. A plasma etching technique similar to that described in reference 4 was used. Etched specimens were sputter coated with 10 nm of palladium, and then examined in a scanning electron microscope equipped with an energy dispersive x-ray spectrometer (XEDS).

Transmission Electron Microscopy (TEM)

For TEM, fibers were cast and vacuum degasssed in a mixture of epoxy and 6 μm alumina powder in a 3 mm diameter by 20 mm long brass tube. After the mixture hardened, ~1 mm thick disks were sectioned using a diamond saw. The disks were mechanically ground from both sides, dimpled, and ion-beam thinned. Details of the specimen preparation technique are described elsewhere (ref. 5). For conventional and analytical TEM, a Phillips Model 400T, operating at 120 kV was used.

RESULTS

Strength After Exposure

The room-temperature tensile strength results for SCS-6 fibers in the as-received condition and after heat-treatment in 0.1 MPa argon for 1, 10, 100, 200, and 400 hr at temperatures to 2100 °C are shown in figure 2. Each data point represents an average of ten to fifteen individual tests, and the error bars cover ± 1 standard deviation. Figure 2 shows that the as-fabricated tensile strength value of 4.0 GPa was maintained after 1 hr heat-treatment at 1400 °C. Beyond this temperature, the strength decreased continuously with increasing temperature up to 1800 °C and, then appeared to reach a plateau. The strength generally decreased with increasing time of exposure, but the heat treatment temperature had a greater influence on the strength degradation than the time of exposure. The temperature at which strength degradation initiated also depended on the exposure time. For example, the fibers heat treated for 400 hrs at $T < 1300$ °C retain their strength, whereas strength degrades in 1 hr if the temperature is raised above 1400 °C.

To determine the influence of heat treatment on growth related residual strain and microstructure, and to determine the flaw population responsible for fiber failure, x-ray analysis, microstructural characterization, and fracto-graphy were performed. X-ray diffractometer traces of the heat-treated fibers revealed sharpening of the diffraction peaks with increasing temperature of exposure above 1400 °C (fig. 3). The crystal structure of the fiber remained β-SiC at temperatures to 2000 °C, and at 2100 °C, partial transformation to α-SiC was noticed. The sharpening of diffraction peaks suggests annealing of lattice strains, or grain coarsening.

In most cases, the as-received fibers, and the fibers heat treated up to 1500 °C broke into multiple pieces upon tensile testing. Therefore unequivocal identification of the critical flaw responsible for the primary fracture became difficult. However, fractographic analysis of some of the retained primary fracture surfaces indicates that the as-fabricated SCS-6 fibers failed from a flaw at the core/sheath boundary, and those fibers heat-treated at 1700 °C for 1 hr failed from a flaw closer to the outer surface of Region B of the SiC sheath (fig. 4). But the nature of the flaw could not be determined even at high magnification.

Figure 5 shows SEM photographs of the cross-sections of the as-received SCS-6 fibers and those heat treated at 1600, 1700 and 1800 °C for 1 hr, and 1400 °C for 400 hr for in 0.1 MPa argon. According to this figure, at 1600 °C, a reaction zone (appears as relatively smoother zone in the photographs) is observed at the interface of the carbon-rich surface coating and the outer zone of the fiber containing near-stoichiometric SiC grains. The graininess seen on the left side of the reaction zone is due to differential removal of material during plasma etching. With increasing temperature of exposure and time, the reaction zone thickness increased. At 1800 °C and above exaggerated grains started growing from the reaction zone. At 2000 °C, nearly 90 percent of the outer zone (Region B) was covered with exaggerated grains.

The effect of heat treatment on the microstructure of four major zones of the fiber namely, the carbon core, carbon-rich SiC zone, near stoichiometric SiC zone, and carbon-rich surface coating was analyzed using a TEM. The carbon core retained its turbostratic structure at all exposure conditions used in the current study. In the as-received condition, the carbon-rich SiC zones—Regions C, D, and E in figure 1—contained SiC columnar grains extending in the radial direction with <111> preferred orientation. Upon heat treatment at temperatures above 1600 °C, the SiC grains in these zones showed slight spheroidization, and the excess carbon present around the SiC grains redistributed (fig. 6). But these zones appeared to resist recrystallization and grain growth even after heat treatment to 2100 °C.

On the other hand, most of the microstructural changes were observed in the near-stoichiometric SiC zone (Region B) and the carbon-rich surface coating (Region A). With increasing heat treatment temperature above 1400 °C, the recrystallization of SiC grains initiated at the interface between the carbon-rich surface coating and the SiC sheath containing near stoichiometric SiC grains (This layer corresponds to the relatively smoother zone seen in figure 5). The recrystallized region grew radially inward towards the core with increasing time of exposure at a given temperature (fig. 5). At the boundaries of the recrystallized grains small pores of size ~50 nm were noticed (fig. 7). With increasing recrystallized zone thickness, however, the average pore size remained nearly the same. The recrystallized grains exhibited a more random crystallographic orientation than the {111} oriented as-grown grains. Apart from pores, silicide particles were also seen at the boundary between the recrystallized and unrecrystallized region of the fibers heat-treated above 1700 °C. XEDS analysis showed that these particles are complex silicides of Fe, Cr, Ni, and Ti (fig. 8).

The carbon-rich surface coating of the as-produced fiber contained a fine dispersion of SiC particles in the turbostratic carbon matrix (fig. 9(a)). Because the outer region of the coating thinned faster than the inner region during ion milling, the effect of heat treatment on this region of the coating could not always be analyzed. The SiC particles closer to the SiC sheath were found to coarsen during heat treatment. A typical microstructure of the coating on a fiber heat treated at 1800 °C for 1 hr is shown in figure 9 (b).

KINETICS OF RECRYSTALLIZATION ZONE GROWTH AND STRENGTH DEGRADATION

The effect of heat treatment on the thickness of recrystallized region of the outer zone of the SiC sheath was measured, and the results are presented in table I. Each value and its associated ±1 standard deviation represents an average of at least twenty individual measurements. Figure 10 shows plots of the square of the recrystallization zone thickness, h^2 versus exposure time, t, for the fibers heat treated at different temperatures. This plot yields a series of straight lines suggesting that growth of the recrystallization zone follows parabolic rate kinetics; that is, $h^2 = K_h t$, where K_h is the growth rate parameter. Typically, the amount of recrystallization as a function of time for a given temperature should yield a sigmoidal curve. In the present case however, only 5 to 7 percent of the near-stoichiometric SiC zone (Region B) recrystallizes before exhibiting exaggerated grain growth. Therefore, we analyzed the kinetics of early stages of recrystallization and in this stage parabolic rate kinetics follows the data. A plot of the logarithm of the slopes of the growth rate parameter of figure 10 as a function of the reciprocal of the absolute temperature also yields a straight line (fig. 11). This suggests that zone growth is thermally activated and the growth rate parameter obeys the relation $K_h = K^0_h \exp^{-Q/RT}$, where Q is the Arhennius activation energy for growth, R is the universal gas constant (8.314 J/mole), and T is the absolute temperature. From the slope of the line in the figure 11, the average activation energy for the growth of the recrystallization zone is calculated to be ~370 kJ/mole.

Apart from the kinetics of the recrystallization zone, the kinetics of SiC particle growth in the carbon-rich surface coating were also studied. In table II, the average diameter and area fraction of SiC particles in the as-received condition and after 1 hr exposure at 1400, 1700 and 1800 °C are shown. Assuming parabolic growth, plots of the square of the particle diameter, D^2, versus exposure time, t and the growth rate parameter, K_D, versus reciprocal of the absolute temperature are shown in figure 12. The calculated average activation energy for this process is ~320 kJ/mole.

To determine whether a correlation exists between the fiber strength and the recrystallization zone parameter, the tensile strength of heat treated fibers is plotted against the inverse of the square root of the recrystallization zone thickness (fig. 13). Here it is assumed that Griffith's Law applies; that is $\sigma = K_{IC}/(h)^{1/2}$ where σ is the fiber strength, K_{IC} is the fracture toughness of SiC sheath, and h is the strength controlling flaw size which is assumed to be equal to the recrystallized zone thickness. The error bars in both strength and thickness measurements in figure 13 represent ±1 standard deviation. According to this figure, the tensile strength of heat treated fibers remained nearly the same up to a recrystallization zone thickness of 0.5 μm and then it decreased with increasing recrystallization zone thickness. The slope of the linear portion of the curve is ~2.5 $MNm^{-3/2}$. This value is similar to the fracture toughness values (2 to 3.5 $MNm^{-3/2}$) reported for monolithic SiC material (ref. 6).

DISCUSSION

The SCS-6 SiC fibers heat treated in argon showed microstructural changes and strength degradation which increased with increasing temperature and time of exposure above 1300 °C. Degradation appears to be intrinsic and starts from a flaw closer to the outside surface of Region B - at the SiC/carbon-rich coating interface where recrystallization of SiC grains was also observed. From the knowledge of the manufacturing method, microstructure, and heat treatment conditions of the fiber, it is possible to elucidate the reasons for microstructural instability and strength degradation.

As discussed earlier, the SCS-6 fiber consists of a carbon core, several zones of SiC having slightly different morphology and microstructure, and a carbon-rich surface coating. According to the manufacturer (ref. 7), as the SiC grains grow radially on the resistively heated carbon core, the electrical conductivity of the fiber increases, thus lowering the electrical power and deposition temperature of the outer SiC layers. Typically, the temperature at the top end of the reactor where SiC grains are deposited on the carbon core is ~1300 °C, and the temperature at the lower end of the reactor where the carbon-rich coating is deposited on the SiC substrate is ~1150 °C (ref. 7). Since

different regions are deposited at different temperatures, growth related residual stresses are generated in the fiber. Near the surface of the fiber, the residual stresses are compressive and their magnitudes range from 0.5 to 1 GPa (refs. 8 and 9). Also, the lower deposition temperature of the outer layers tends to produce silicon-rich SiC (ref. 10).

The SiC sheath in Region B consists of fine grained, highly faulted SiC grains having an aspect ratio ranging from 5 to 10. The fine grain size indicates relatively high grain boundary surface energy. The growth related residual stresses and the grain boundary surface energy can be reduced when fibers are heated at a temperature above which diffusion of silicon or carbon is significant. Indications of these effects are observed from the x-ray data apart from recrystallization and grain growth seen from the SEM and TEM results. Although recrystallization and grain growth changes the grain size of the fibers, both of these processes may not influence the strength of fibers unless they create flaws that are much more severe and of dimension larger than the pre-existing flaws in the as-produced fiber. That is, the strength of the fiber is controlled by the largest flaw according to Griffith's failure criterion for brittle solids. The fact that the heat treated fibers can develop a recrystallization zone thickness of ~0.5 μm before showing any significant strength degradation suggests that up to this thickness, the flaws created during growth of the recrystallization zone are smaller than the intrinsic flaws present in the as-produced fibers. Close examination of the recrystallization zone reveals that the controlling flaws do not appear to be associated with the recrystallized grains but possibly with the formation of a series of voids in the recrystallization zone, and segregation of complex silicide particles of iron, nickel, chromium, and titanium at the unrecrystallized to recrystallized boundary. Although the size of these voids remains nearly the same under the heat treatment conditions and is comparable to the size of the recrystallized grains, the fact that strength of the fiber decreases with increasing recrystallization zone thickness indicates that the collection of these voids may cumulatively act as a larger flaw of size perhaps equivalent to the recrystallization zone thickness.

The reasons for the void formation in the recrystallization zone and the segregation of silicide particles at the boundary between the recrystallized and the unrecrystallized zones are not clearly understood. A suggested reason for the void formation is due to the outward diffusion of free silicon atoms from the near-stoichiometric Region B into the carbon-rich surface coating. Several pieces of direct and indirect evidence point to the existence of excess silicon in CVD SiC fibers. The microprobe analysis of the cross-section of the as-received fibers conducted in this study shows an increase in the silicon to carbon ratio when traversing from the inner zone to outer zones, suggesting the presence of free silicon in Region B. This conclusion is in agreement with the phase analysis results of Martineau et al. (ref. 11) who found that the inner zone generally contained a few percent of excess carbon, whereas the outer zone was either stoichiometric or slightly silicon-rich. Furthermore, the observation of hysteresis in the thermal expansion and contraction curves of the fiber between 1370 and 1420 °C, and a close match between the activation energy for creep deformation of this fiber (ref. 12) with that of self diffusion of silicon also support the existence of excess silicon in the outer sheath.

Formation of silicides is due to reaction of metallic impurities with SiC grains during heat treatment. It is suspected that these metallic impurities possibly come from the methyltrichlorosilane gas and the stainless steel hardware used for the CVD process (ref. 7).

Assuming the existence of excess silicon in CVD SiC fibers, we can thus explain the formation of voids and strength degradation. The free silicon contained in Region B has an equal probability of diffusing into the inner carbon-rich SiC zones (Regions C, D and E) as well as into the carbon-rich surface coating (Region A). In the early stage, the free silicon diffusing into inner zones will possibly react with the excess carbon present in these zones to form SiC. However, continuation of this reaction is doubtful because this conversion is associated with about a 90 percent increase in volume. Unless this volume expansion is accommodated, silicon and carbon reaction will not continue. On the other hand, diffusion of free silicon through the grain boundaries of the SiC grains into the carbon-rich coating is more feasible. This diffusion is possibly assisted by vacancy or impurity diffusion from the carbon-rich surface coating into the outer layers of Region B which may also explain the existence of silicide particles at the unrecrystallized to recrystallized boundary, and the growth of the recrystallization zone from the interface of the carbon-rich surface coating and SiC substrate.

Apart from the recrystallization of SiC grains in Region B of the SiC sheath, the carbon-rich surface coating also showed coarsening of SiC particles upon heat treatment. In general, coarsening of particles in a matrix can occur by three mechanisms namely; Oswald ripening, dissolution and reprecipitation, and surface diffusion. Of the three mechanisms, the dissolution and reprecipitation mechanism may not operate in the carbon-rich surface coating as this mechanism requires a liquid phase which is non existent under the heat treatment conditions of the fibers.

For the system of dispersed particles of varying size in a medium in which they have some solubility, particle coarsening by Oswald ripening can occur. Here the smaller particles dissolve and the larger ones grow. The

driving force for this mechanism is the reduction of interfacial free energy. In the silicon-carbon system, a very small amount of silicon is soluble in carbon below the melting point of silicon- <0.2 atom % during codeposition of CVD silicon and carbon (ref. 13) - and therefore the solubilty range of silicon in carbon is not even shown in the phase diagram (ref. 14).

Accelerated coarsening due to surface diffusion effects has been reported (ref. 15) in SiC compacts that were heat treated in argon above 1250 °C. These compacts contained contiguous submicron SiC particles and a small amount (<0.5%)of carbon. As a result of coarsening, the compacts showed a reduction in surface area, but not in pore volume. It is also known that during coarsening, the larger particles grow at the expense of the smaller particles, but the total volume or area fraction of the particles remains the same to maintain the mass balance.

As described earlier, the carbon-rich surface coating on the as-processed SCS-6 fibers contains well dispersed SiC particles in a carbon matrix. Upon heat treatment above 1400 °C, the diameter and the area fraction of these particles increases with increasing temperature of exposure (cf. table II). In a dispersed system where interparticle distances are far greater than the particle diameter, particle coarsening cannot occur without its dissociation followed by the diffusion of atomic species through the matrix. It is known that a silicon atom surrounded by carbon atoms has a greater affinity for the formation of SiC than the diffusion of silicon through the carbon matrix. Therefore, dissociation of SiC particles and long range diffusion of silicon through the carbon matrix is thermodynamically unfavorable under 1 atm argon. The fact that the area fraction of the SiC particles increases with increasing temperature suggests that SiC particle coarsening is possibly caused by the silicon coming into the coating from an external source. One likely possibility is that the free silicon from the Region B diffuses outward into the coating through the kernel boundaries of the SiC grains, thus providing a source of silicon for the growth of SiC particles in the carbon-rich surface coating either by Oswald ripening or by a surface diffusion mechanism. However, because of the limited TEM data, it is not clear which mechanism is the dominant one.

The kinetic data indicate that the activation energies for the growth of the recrystallization zone and for the coarsening of SiC particles in the carbon-rich coating are ~370 and 320 kJ/mole, respectively. Nearly the same activation energy value suggests that both processes are probably controlled by the same mechanism. These values, however, are significantly lower than the activation energy values of 600 and 630 kJ/mole for lattice diffusion of silicon (ref. 16) and carbon (ref. 17), respectively in bulk SiC material, and the activation energy value of 494 kJ/mole for grain boundary diffusion for carbon in SiC (ref. 16) ,and the lattice diffusion coefficient value of 430 kJ/mole for silicon in silicon (ref. 18). This suggests that diffusion does not occur by these intrinsic processes, but occurs possibly by assistance from impurity elements such as iron and nickel which are present in the outer fiber layers.

Although recrystallization and grain growth was prevalent in the outer zone, the inner zone which contained carbon-rich silicon carbide seemed to resist grain growth even at temperatures to 2100 °C. This observation is consistent with the general grain growth behavior of monolithic SiC (ref. 19) where carbon is known to inhibit grain growth, and with high resolution TEM study of heat treated SCS-6 fibers by Ning et al. (ref. 20) .

It has been stated earlier that the carbon-rich surface coating on the SiC substrate is applied to improve the as-produced strength of the fibers. This implies that any factors affecting the surface coating should also influence the fiber strength. Even though after high temperature heat treatment in argon the fiber coating shows several changes, results strongly indicate that residual strength of heat treated SCS-6 fibers is controlled by recrystallization zone thickness. Since recrystallization is a thermally activated process, the recrystallization zone thickness and hence the residual strength of the fibers for any heat treatment condition can be predicted from the time-temperature relationship for the growth of the reaction zone, and from the strength to recrystallization zone thickness plot, provided the recrystallization zone thickness is greater than 0.5 μm. For example, this calculation shows that to retaining a 4 GPa strength in SCS-6 fibers after 10,000 hr exposure in argon, the heat treatment temperature should not exceed 1100 °C.

SUMMARY OF RESULTS

The temperature and time effects on the room-temperature tensile strength of a CVD SiC fiber (SCS-6) exposed to 0.1 MPa argon have been determined. The important findings are as follows.

(a) The CVD SiC fibers show strength degradation above 1300 °C after 400 hr exposure.

(b) Recrystallization and grain growth of the outer zone SiC grains is observed in fibers showing strength degradation. Fiber strength varies inversely with the recrystallization zone thickness.

(c) Inner zone SiC grains with carbon-rich boundaries show greater resistance to recrystallization than the outer grains.

(d) X-ray data show that β-SiC composition is stable to ~2000 °C.

(e) The CVD SiC fibers contain Fe, Cr, Ni, and Ti impurities which appear to be confined to the outer zone and may play a role in the recrystallization process and in strength degradation.

(f) Using the recrystallization kinetics, and the strength and recrystallization zone thickness relationship, we predict that the as-fabricated strength of SCS-6 fibers can be retained only up to ~1100 °C after 10,000 hr exposure in argon and under zero stress conditions.

CONCLUSION

Current study clearly suggests that thermal stability of SCS-6 fibers is controlled by the near-stoichiometric region. Upon high temperature exposure in argon, this region shows recrystallization of SiC grains, growth of voids and formation of silicide particles. All these microstructural changes are due to diffusion of free silicon and impurity elements in the outer layers of the SiC sheath. By eliminating free silicon and impurities or by processing CVD SiC with small amount of carbon at the grain boundaries the thermal stability of CVD SiC fibers should be improved.

ACKNOWLEDGMENTS

The authors wish to thank T.A. Leonhardt for cermographic work and R.G. Garlick for X-ray diffraction studies.

REFERENCES

1. F.W. Wawner, A.Y. Teng, and S.R. Nutt, "Microstructural Characterization of SiC (SCS) Filaments," SAMPE Q., **4** [3], pp. 39–45 (1983).
2. X.J. Ning and P. Pirouz, "The Microstructure of SCS-6 SiC Fiber," J. Mater. Res., **6**, pp. 2234–48 (1991).
3. R.T. Bhatt and D.R. Hull, "Strength and Microstructural Stability of a SiC Fiber in Argon Environment," Ceram. Eng. Sci. Proc., **12**, pp. 1832–1844 (1991).
4. D.R. Hull, T.A. Leonhardt, and W.A. Sanders, "Plasma Etching a Ceramic Composite," in Structure-Property Relationships and Correlations with the Environmental Degradation of Engineering Materials, D.R. Wheeler, G.W.E. Johnson, D.V. Miley, and M.H. Louthan, Jr., Eds., Microstructural Science, **19**, pp. 671–679 (1992).
5. R. Koch and A.F. Marshall, "Specimen Preparation for Transmission Electron Microscopy of Materials II," Mater. Res. Soc. Symp. Proc., **199**, pp. 145–152 (1990).
6. N.L. Hecht, D.E. McCullun, and G.A. Graves, "Investigation of Selected Silicon Nitrides and Silicon Carbide Ceramics," Ceram. Eng. Sci. Proc., **9** [9-10], pp. 1313–32 (1988).
7. H. Debolt and V.K. Krukonis, "Improvement of Manufacturing Methods for the Production of Low Cost Silicon Carbide Filament," Air Force Contract F33615–72–C–1177, Report No. AFML–TR–73–140 (1973).
8. R.W. Rice and K.R. McKinney, "Residual Stresses and Scaling CNTD SiC to Larger Sizes," J. Mat. Sci. Lett. **1**, pp. 159–162 (1982).
9. D.R. Behrendt, "Growth Related Residual Stresses in CVD SiC (SCS-6) Fibers," in press.
10. J.R. Weiss and R.J. Diefendorf, "Chemical Vapor Deposition," edited by G. Wakefield and J.M. Blocher, Jr, (Electrochemical Society, Princeton, New Jersey, 1973) p. 448.
11. P. Martineau, M. Lahaye, R. Pailler, R. Naslain, M. Couzi, and F. Creuge, "SiC Filament/Titanium Matrix Composites Regarded as Model Composites-Part 1 Filament Microanalysis and Strength Characterization," J. Mater. Sci, **19**, p. 2731 (1984).
12. J.A. DiCarlo, "Creep of Chemically Vapour Deposited SiC Fibers," J. Mater. Sci, **21**, pp. 217–224 (1985).
13. S. Marinkovic, C. Suznjevic, I. Dezarvo, A. Mihajlovic, and V. Cerovic, "Simultaneous Chemical Vapor Deposition of Silicon and Carbon," Carbon, **8**, pp. 283–295 (1970).
14. R.W. Olesinski and G.J. Abbaschian, Bull. Alloy Phase Diagrams, **5** (5) 1984.

15. C. Greskovich, and J.H. Rosolowski, "Sintering of Covalent Solids," J. Am. Ceram. Soc., **59**, pp. 336–343 (1976).
16. M.H. Hon, R.F. Davis, and D.E. Newbury, "Self-diffusion of ^{30}Si in Polycrystalline β-SiC," J. Mat. Sci., **15**, pp. 2073–2080 (1980).
17. M.H. Hon and R.F. Davis, "Self-diffusion of ^{14}C in Polycrystalline β-SiC," J. Mat. Sci., **14**, pp. 2411–2421 (1979).
18. C.J. Smithells and E.A. Brandes, (editors), "Metals Reference Book," 5th ed. (Butterworths, London, 1976) p. 868
19. S. Prochazka, "The Role of Boron and Carbon in the Sintering of SiC," Special Ceramics, #6, edited by D. Popper. Stoke-On-Trent,(B. Ceram. R.A., 1975) p. 171.
20. X.J. Ning, P. Pirouz, and R.T. Bhatt, "The Effect of High Temperature Annealing on the Microstructure of SCS-6 SiC Fiber," Mater. Res. Soc. Symp. Proc., **250**, pp. 187–92 (1992).

TABLE I.—SUMMARY OF RECRYSTALLIZATION ZONE THICKNESS DATA FOR SCS–6 FIBERS

Heat treatment temperature, K	Recrystallization zone thickness after heat treatment, μm				
	1 h	10 h	100 h	200 h	400 h
1473	------	------	------	0.23±0.06	0.38±0.05
1573	------	0.16±0.02	0.29±0.04	0.36±0.06	0.48±0.02
1673	0.53±0.16	------	1.36±0.17	1.55±0.17	2.37±0.16
1773	0.76±0.11	------	1.94±0.23	------	------
1873	0.82±0.12	1.5	------	------	------
1873	1.29±0.18	2.17±0.19	------	------	------

TABLE II.—SUMMARY OF SiC PARTICLE COARSENING DATA FOR CARBON-RICH COATING OF SCS–6 FIBER

Heat treatment temperature, K	Average SiC particle diameter after 1 hr treatment, μm	Area fraction of SiC particles, percent
298	0.007±0.003	Not measured
1673	0.012±0.006	2±0.75
1973	0.038±0.011	13±0.5
2073	0.053±0.02	15±0.3

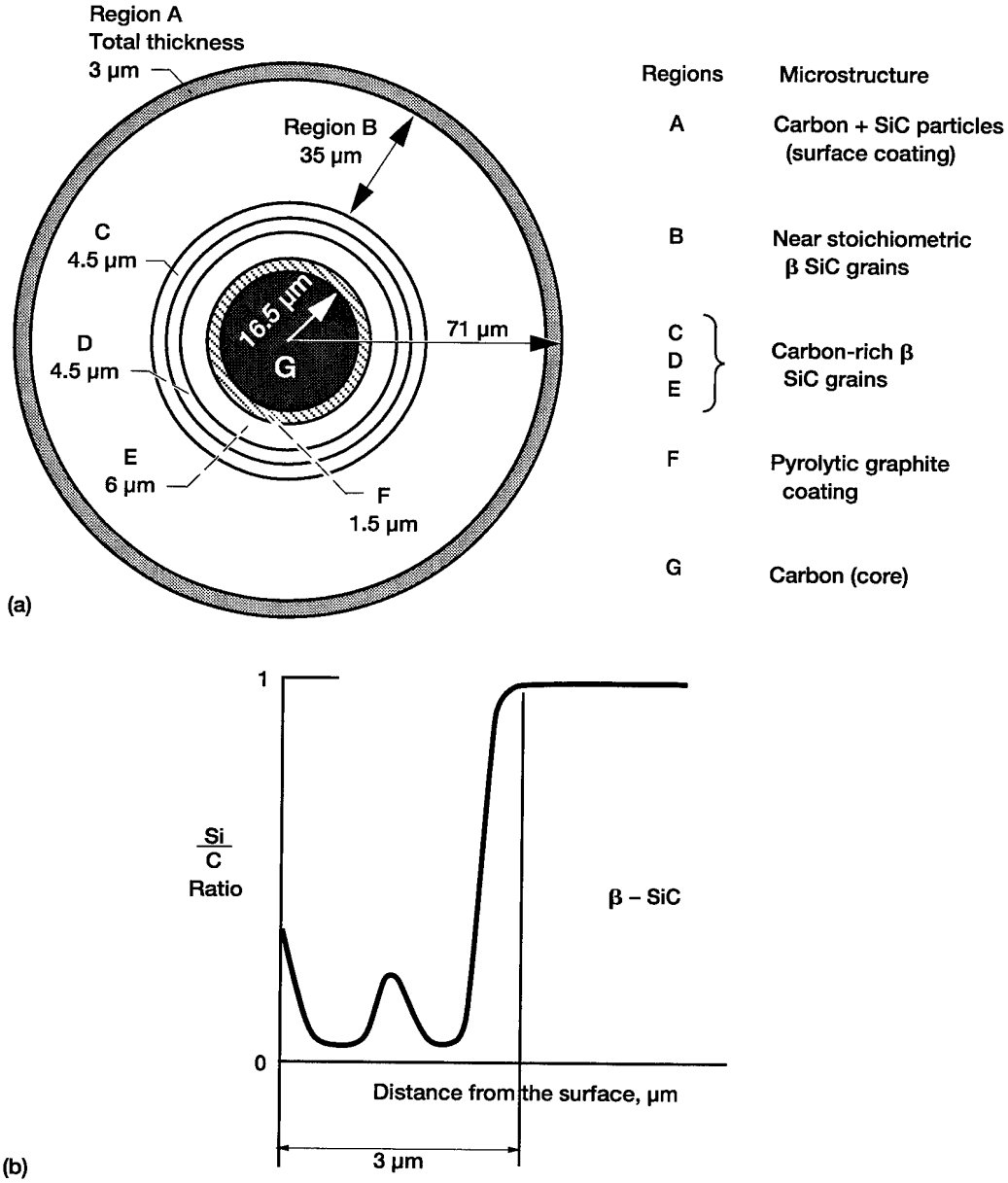

Figure 1.—(a) Schematic showing CVD SCS-6 SiC fiber cross section. (b) Variation of Si/C ratio in the carbon-rich surface coating.

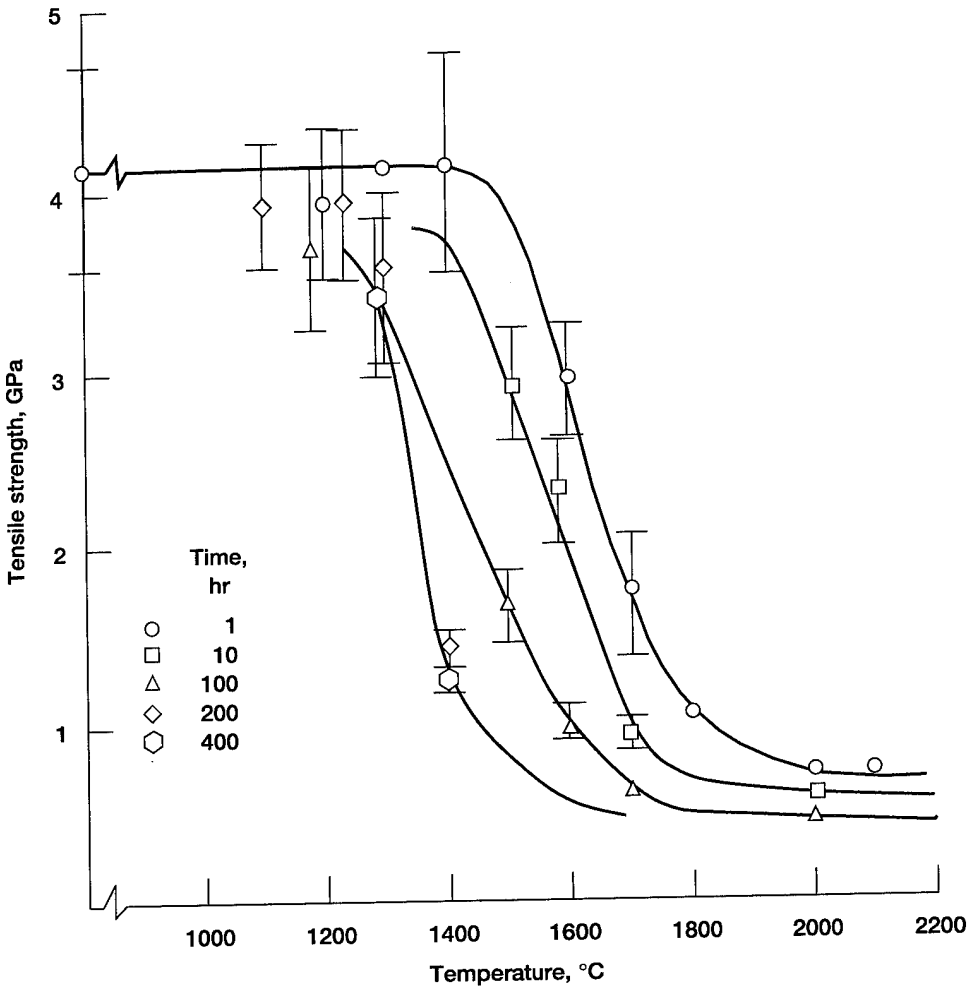

Figure 2.—Effects of temperature and time on the room-temperature tensile strength of SCS-6 fibers heat-treated in 0.1 MPa argon.

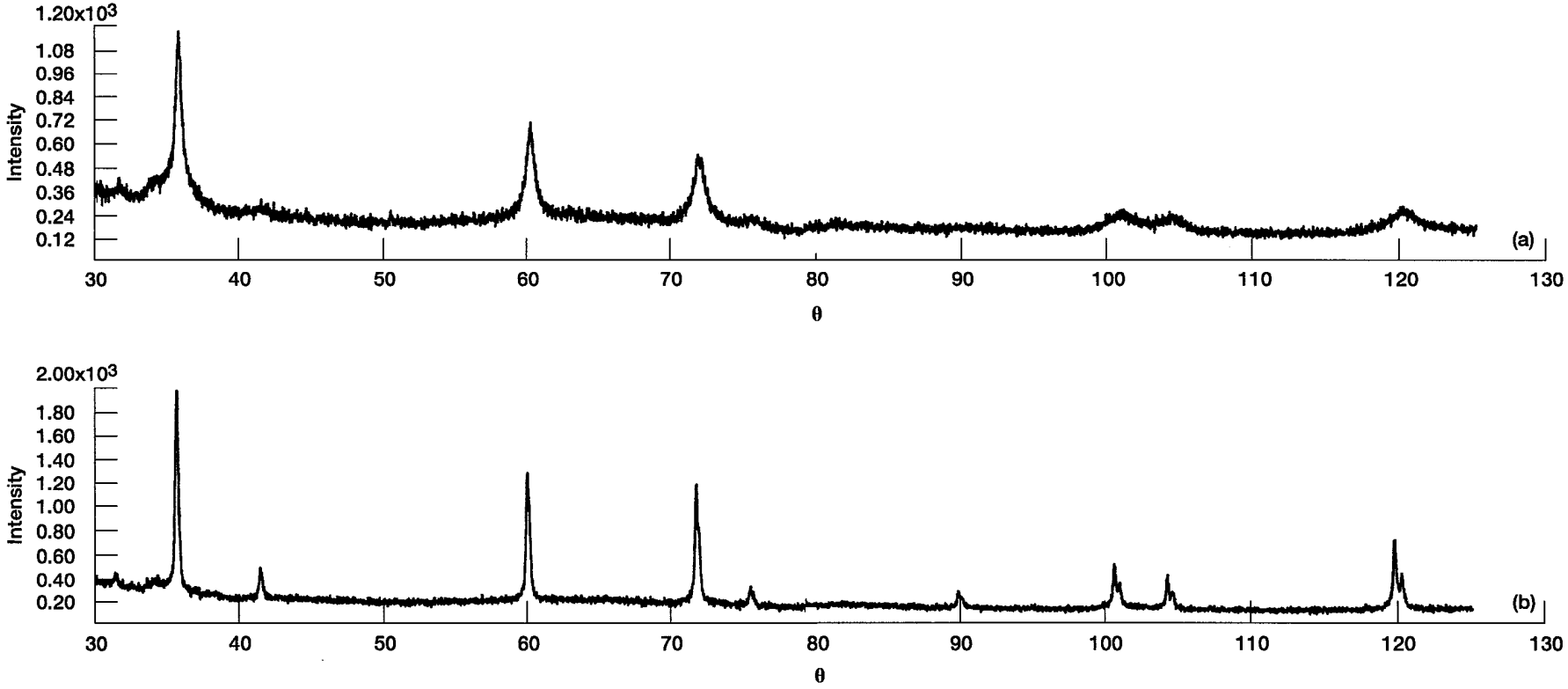

Figure 3.—Effect of heat treatment on X-ray diffraction peaks of SCS-6 fibers: (a) As-received; (b) Heat-treated at 2000 °C for 1 hr.

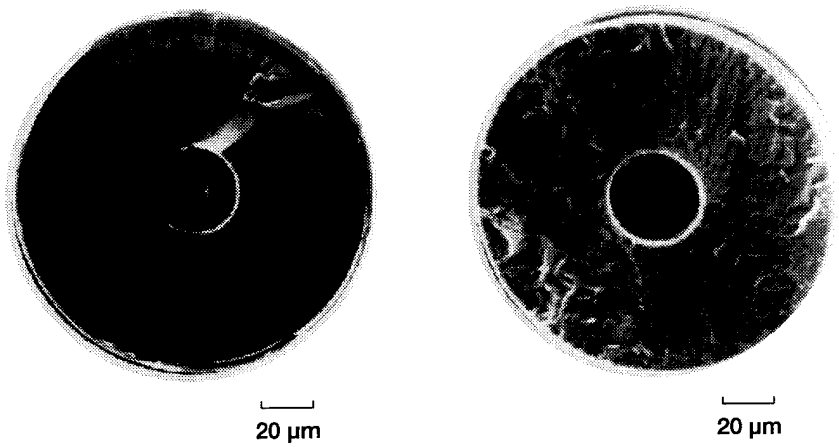

Figure 4.—SEM photographs of SCS-6 fibers showing tensile fracture origin: (a) As-fabricated; (b) Heat-treated at 1700°C for 1 hr.

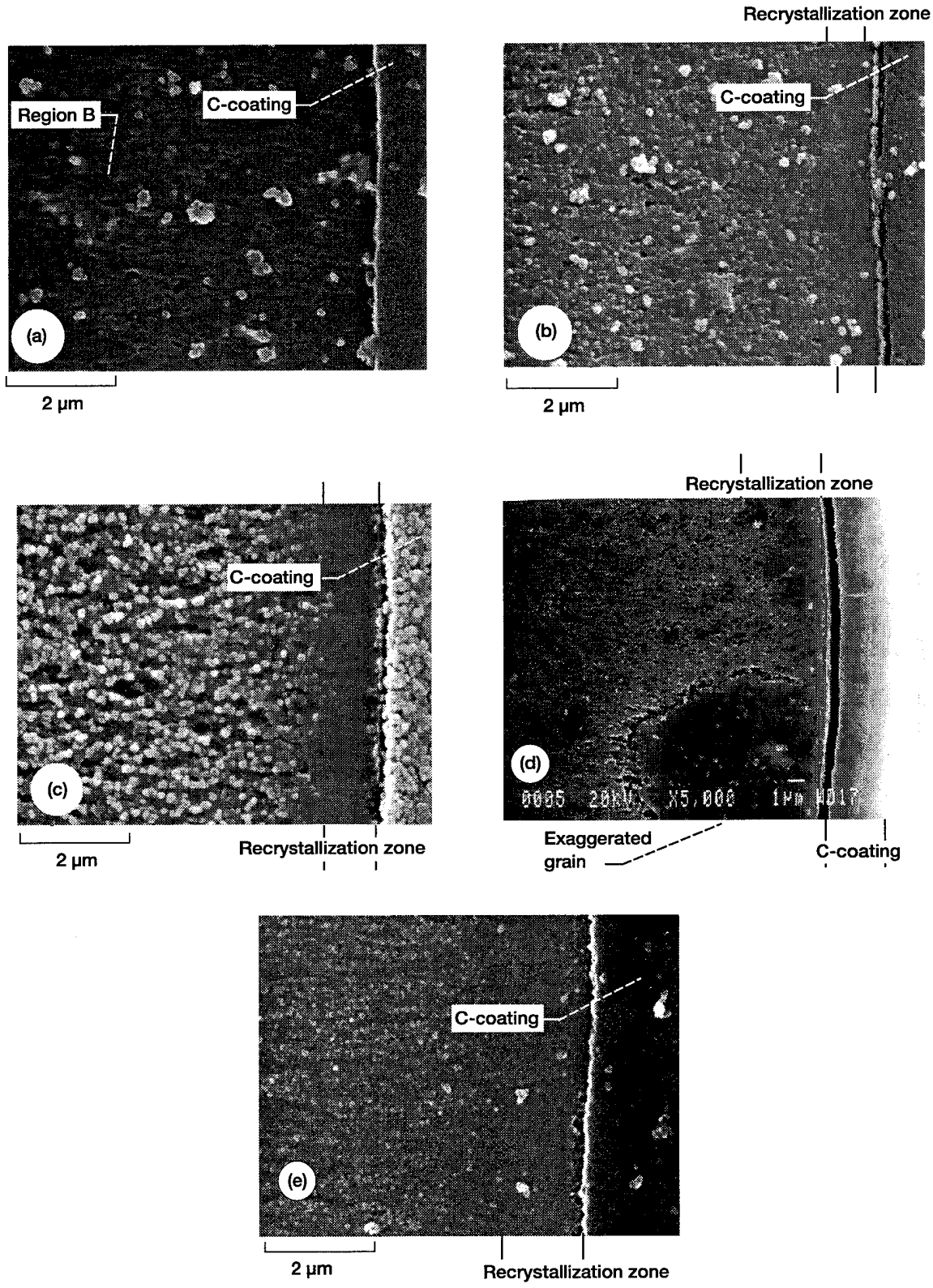

Figure 5.—SEM photographs of the etched cross-sections of SCS-6 fibers showing growth of a smooth zone and grain growth in Region B. (a) As-received; After heat-treatment in 0.1 MPa argon at (b) 1600 °C (c) 1700 °C (d) 1800 °C for 1 hr, and (e) 1400 °C for 400 hr, respectively.

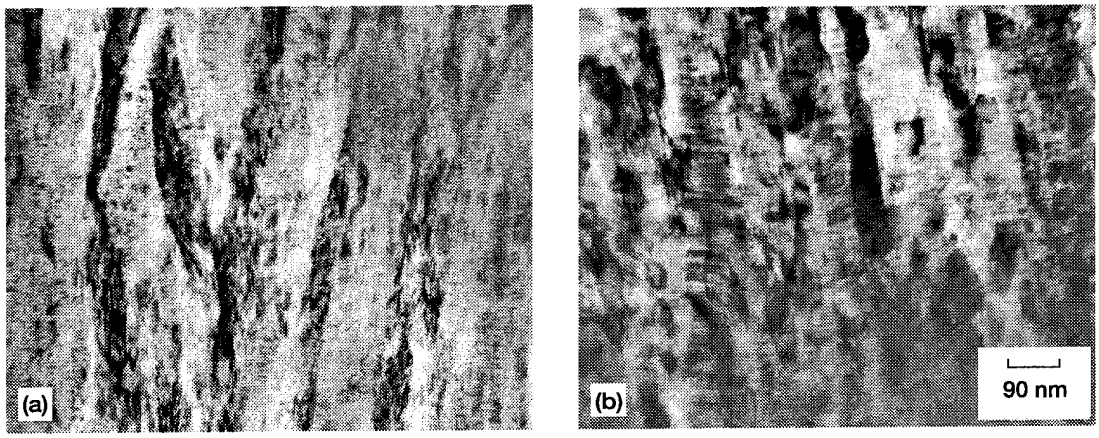

Figure 6.— TEM micrographs of the carbon-rich SiC zone (Region D); (a) As-received; (b) After 1 hr heat treatment in argon at 1800 °C.

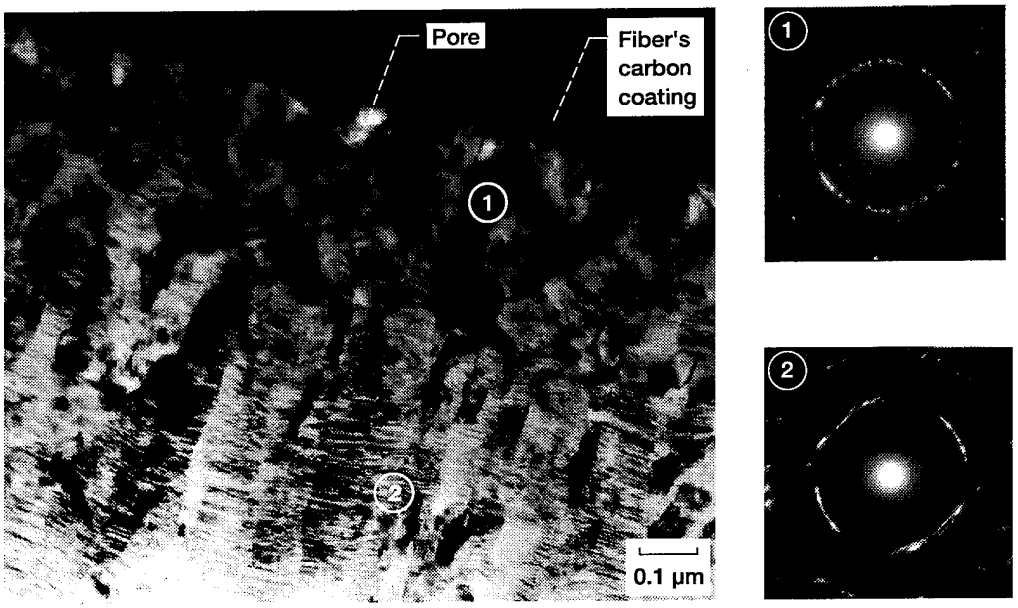

Figure 7.—TEM micrograph of the near stoichiometric zone (Region B) after 200 hr heat-treatment in argon at 1400 °C showing recrystallized region, and pores.

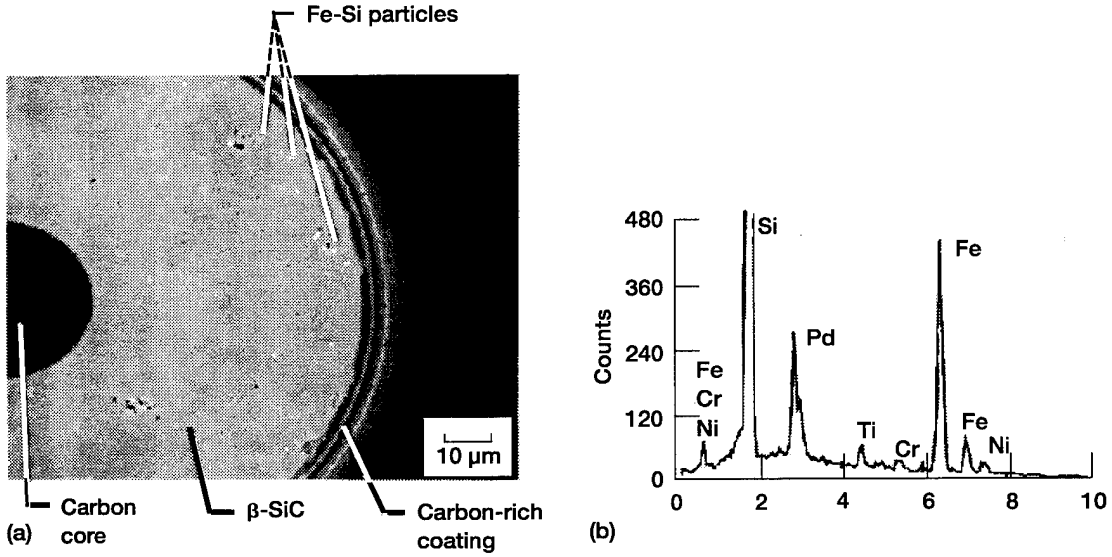

Figure 8.—(a) SEM photograph of a cross-section of SCS-6 fiber heat treated for 1 hr in argon at 2000 °C showing particles in the outer zone. (b) XEDS analysis of the particles. Palladium (Pd) was deposited to provide conductivity.

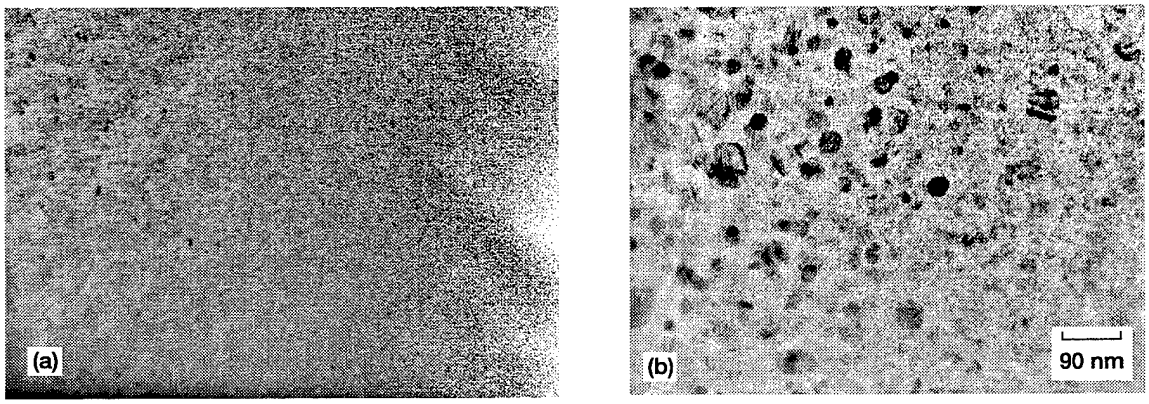

Figure 9.—TEM micrographs showing effect of heat treatment on the carbon-rich surface coating (Region A) of SCS-6 fiber: (a) As-received; (b) After heat-treatment at 1800 °C in argon for 1 hr.

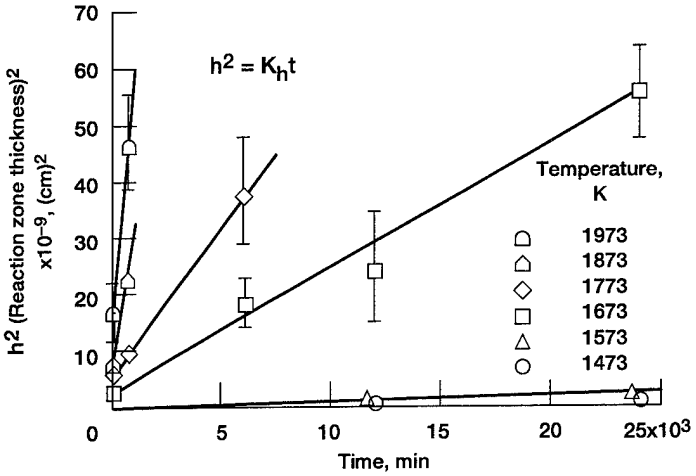

Figure 10.—Growth of the square of the recrystallization zone thickness with exposure time for SCS-6 fibers heat-treated in 0.1 MPa argon.

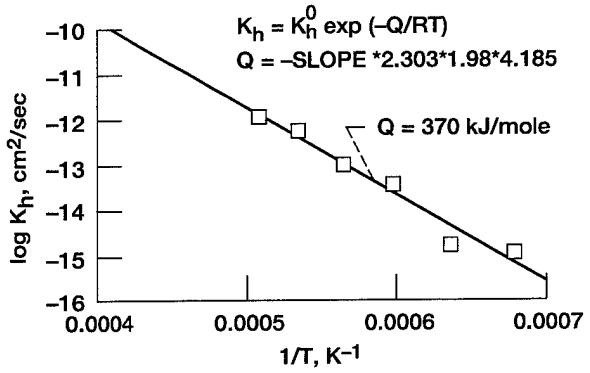

Figure 11.—Variation of the slope of the recrystallization zone growth rate with reciprocal absolute temperature for SCS-6 fibers heat-treated in argon.

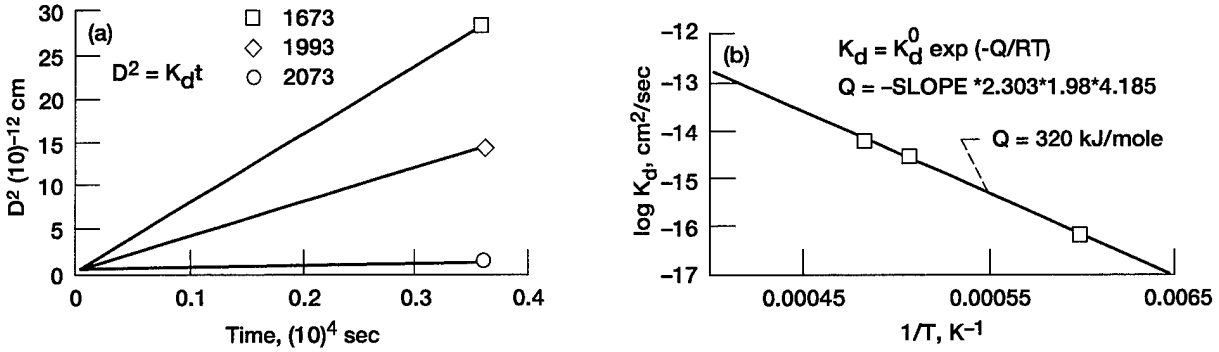

Figure 12.—Kinetics of SiC particle coarsening: (a) Variation of square of the average SiC particle diameter with exposure time; (b) Variation of the slope of the particle growth isotherm with the reciprocal of absolute temperature.

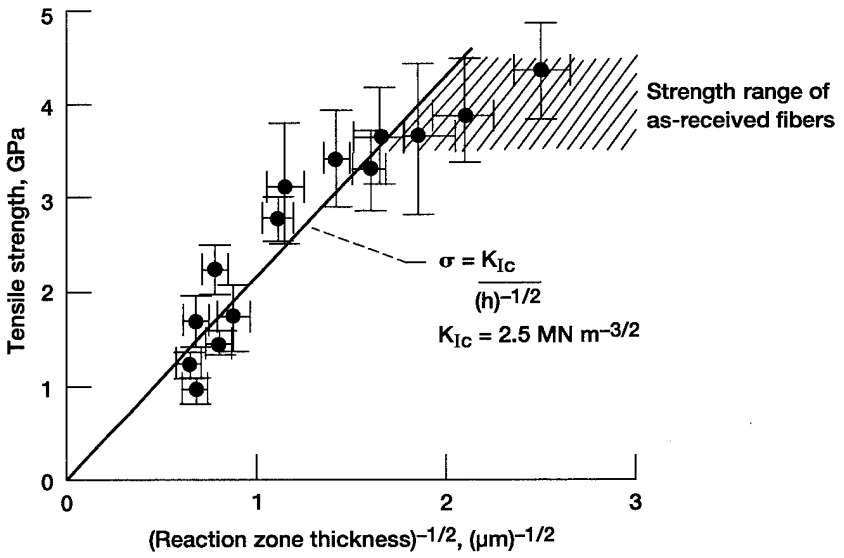

Figure 13.—Variation of room temperature tensile strength with recrystallization zone thickness for SCS-6 fibers heat-treated in argon.

REPORT DOCUMENTATION PAGE

Form Approved
OMB No. 0704-0188

1. AGENCY USE ONLY (*Leave blank*)	2. REPORT DATE	3. REPORT TYPE AND DATES COVERED
	May 1996	Technical Memorandum

4. TITLE AND SUBTITLE
Strength Degrading Mechanisms for CVD SCS–6 SiC Fibers in Argon Environments

5. FUNDING NUMBERS
WU–510–01–10
1L161102AH45 or
1L162211A47A

6. AUTHOR(S)
Ramakrishna T. Bhatt and David R. Hull

7. PERFORMING ORGANIZATION NAME(S) AND ADDRESS(ES)
NASA Lewis Research Center
Cleveland, Ohio 44135–3191
and
Vehicle Propulsion Directorate
U.S. Army Research Laboratory
Cleveland, Ohio 44135–3191

8. PERFORMING ORGANIZATION REPORT NUMBER
E–10122

9. SPONSORING/MONITORING AGENCY NAME(S) AND ADDRESS(ES)
National Aeronautics and Space Administration
Washington, D.C. 20546–0001
and
U.S. Army Research Laboratory
Adelphi, Maryland 20783–1145

10. SPONSORING/MONITORING AGENCY REPORT NUMBER
NASA TM–107169
ARL–TR–1061

11. SUPPLEMENTARY NOTES
Prepared for the 17th Annual Conference on Composites and Advanced Ceramics sponsored by the American Ceramic Society, Cocoa Beach, Florida, January 15–19, 1993. Ramakrishna T. Bhatt, Vehicle Propulsion Directorate, U.S. Army Research Laboratory, Lewis Research Center, Cleveland, Ohio; David R. Hull, NASA Lewis Research Center. Responsible person, Ramakrishna T. Bhatt, organization code 5130, (216) 433–5513.

12a. DISTRIBUTION/AVAILABILITY STATEMENT
Unclassified - Unlimited
Subject Category 27
This publication is available from the NASA Center for Aerospace Information, (301) 621–0390.

12b. DISTRIBUTION CODE

13. ABSTRACT ***(Maximum 200 words)***

The room temperature tensile strengths of chemically vapor deposited SCS-6 silicon carbide fibers were measured after 1 to 400 hr heat-treatments in 0.1 MPa argon at temperatures to 2100 °C. The fibers heat treated for 1 hr above 1400 °C and those heat treated for 400 hr above 1300 °C showed strength degradation. Scanning and transmission electron microscopic examination of the degraded fibers showed formation of a recrystallization region within the outer zone of the Sic sheath and the growth of SiC particles in the carbon-rich surface coating. The activation energies for the growth of the recrystallization region and the SiC particles were ~370 KJ/mole and ~320 KJ/mole, respectively. Strength of the fibers was found to vary as an inverse function of the recrystallized zone thickness.

14. SUBJECT TERMS
SiC fibers; Tensile strength; Microstructure

15. NUMBER OF PAGES
20

16. PRICE CODE
A03

17. SECURITY CLASSIFICATION OF REPORT	18. SECURITY CLASSIFICATION OF THIS PAGE	19. SECURITY CLASSIFICATION OF ABSTRACT	20. LIMITATION OF ABSTRACT
Unclassified	Unclassified	Unclassified	